Detection of a New Substrate-Derived Radical during Inactivation of Ribonucleotide Reductase from *Escherichia coli* by Gemcitabine 5′-Diphosphate†

Wilfred A. van der Donk,‡ Guixue Yu,§ Lucy Pérez, Raylene J. Sanchez, and JoAnne Stubbe*

Departments of Chemistry and Biology, Massachusetts Institute of Technology, Cambridge, Massachusetts 02139

Vicente Samano and Morris J. Robins*

Chemistry Department, Brigham Young University, 225 Eyring Science Center, P.O. Box 24672, Provo, Utah 84602-4672

Received December 1, 1997; Revised Manuscript Received February 25, 1998

ABSTRACT: Ribonucleotide reductases (RNRs) play a central role in replication and repair by catalyzing the conversion of nucleotides to deoxynucleotides. Gemcitabine 5′-diphosphate (F_2CDP), the nucleoside of which was recently approved by the FDA for treatment of pancreatic cancer, is a potent mechanism-based inhibitor of class I and II RNRs. Inactivation of the *Eschericia coli* class I RNR is accompanied by loss of two fluorides and one cytosine. This RNR is composed of two homodimeric subunits: R1 and R2. R1 is the site of nucleotide reduction, and R2 contains the essential diferric−tyrosyl radical cofactor. The mechanism of inactivation depends on the availability of reductant. In the presence of reductant [thioredoxin (TR)/thioredoxin reductase (TRR)/NADPH or dithiothreitol], inhibition results from R1 inactivation. In the absence of reductant with prereduced R1 and R2, inhibition results from loss of the essential tyrosyl radical in R2. The same result is obtained with C754S/C759S-R1 in the presence of TR/TRR/NADPH. In both cases, tyrosyl radical loss is accompanied by formation of a new stable radical (0.15−0.25 equiv/RNR). EPR studies in ^2H_2O, with [U-^{2}H]R1, and examination of the microwave power saturation of the observed signal, indicate by process of elimination that this new radical is nucleotide-based. In contrast to all previously investigated 2′-substituted nucleotide inhibitors of RNR, inactivation is not accompanied by formation of a new protein-associated chromophore under any conditions. The requirement for reductant in the R1 inactivation pathway, the lack of chromophore on the protein, the loss of two fluoride ions, and the stoichiometry of the inactivation all suggest a unique mechanism of RNR inactivation not previously observed with other 2′-substituted nucleotide inhibitors of RNR. This unique mode of inactivation is proposed to be responsible for its observed clinical efficacy.

The nucleoside analogue gemcitabine (2′,2′-difluoro-2′-deoxycytidine) is a potent antitumor agent which recently has been approved for the treatment of non-small cell lung cancer in Europe and pancreatic cancer in the United States (*1*, *2*). Previous studies on the metabolism of gemcitabine have demonstrated that this compound is a prodrug that is converted to the corresponding 5′-diphosphate and triphosphate that are the therapeutically active agents (*3*−*5*). These metabolites have been shown to inhibit two cellular processes required for DNA biosynthesis, nucleotide reduction (*6*, *7*) and replicative DNA chain elongation (*8*). In a previous preliminary study, we showed that the 5′-diphosphate of gemcitabine (**1**) acts as a potent mechanism-based inhibitor of ribonucleoside diphosphate reductase (RDPR)[1] from *Escherichia coli* (*9*). In this work, we report the results of detailed studies on the interaction of **1** with RDPR. These studies have established that an unusually stable substrate-based radical is formed during enzyme inactivation. Furthermore, the characteristics of this inhibition process are very different from those of previously studied 2′-substituted nucleotide analogues and suggest a unique mode of action that may be in part responsible for the clinical efficacy of gemcitabine.

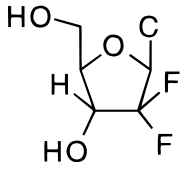

gemcitabine

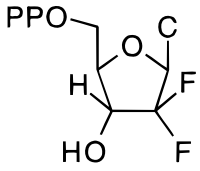

1

† This research was supported by a grant from the National Institutes of Health to J.S. (GM-29595) and by a postdoctoral fellowship to W.A.v.d.D. from the Jane Coffin Childs Memorial Fund for Medical Research (Project 61-960).

* Corresponding author. Telephone: (617) 253-1814. Fax: (617) 258-7247. E-mail: stubbe@mit.edu.

‡ Present address: Department of Chemistry, University of Illinois at Urbana−Champaign, Urbana, Illinois 61801.

§ Present address: Cubist Pharmaceuticals, 24 Emily St., Cambridge, Massachusetts 02139.

[1] Abbreviations: ATP, adenosine 5′-triphosphate; CDP, cytidine 5′-diphosphate; DTT, dithiothreitol; EDTA, ethylenediaminetetraacetic acid; FMCDP, 2′-fluoromethylene-2′-deoxycytidine 5′-diphosphate; Hepes, *N*-(2-hydroxethyl)piperazine-*N*′-2-ethanesulfonic acid; NADPH, reduced β-nicotinamide adenine dinucleotide phosphate; N_3UDP, 2′-azido-2′-deoxyuridine 5′-diphosphate; RDPR, ribonucleoside 5′-diphosphate reductase; RNRs, ribonucleotide reductases; SA, specific activity; TR, thioredoxin; Tris, tris(hydroxymethyl)aminomethane; TRR, thioredoxin reductase; Y•, tyrosyl radical on residue 122 of the R2 subunit.

S0006-2960(97)02935-8 CCC: $15.00
Published on Web 04/14/1998

Scheme 1

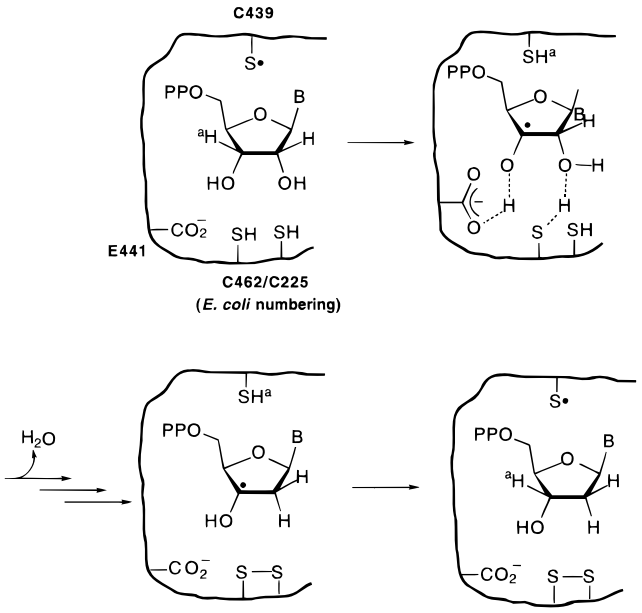

The *E. coli* ribonucleoside diphosphate reductase (RDPR) is composed of two homodimeric subunits (R1 and R2) and serves as the prototype of the mammalian enzyme. R1 contains the active site for reduction of both purine and pyrimidine substrates, and five cysteines that are required for catalysis (*10*−*13*). R2 contains the essential tyrosyl radical ($Y_{122}^{\bullet}$)−diferric cluster cofactor which is thought to generate a thiyl radical at cysteine 439 in the active site on R1 by a series of coupled electron and proton transfers (*13*−*15*). This thiyl radical then initiates the actual reduction process by abstraction of the 3′-hydrogen atom from the substrate. The putative substrate radical generated then loses water and is reduced with concomitant oxidation of two cysteines, Cys225-R1 and Cys462-R1, in the active site of the enzyme (Scheme 1) (*13*, *16*). The thiyl radical on Cys439 is then regenerated by hydrogen atom transfer to the 3′-deoxyribonucleotide radical providing the reduction product.

To allow for subsequent turnovers, the disulfide between Cys225 and Cys462 needs to be reduced. In vitro, this can be achieved using an enzymatic reduction system consisting of thioredoxin (TR), thioredoxin reductase (TRR), and NADPH. On the basis of biochemical (*11*) and site-directed mutagenesis studies (*13*), it has been proposed that thioredoxin delivers the reducing equivalents by dithiol interchange to Cys754 and Cys759 which the structure indicates are on the outside of R1 and not detectable due to thermal lability (eq 1) (*15*).

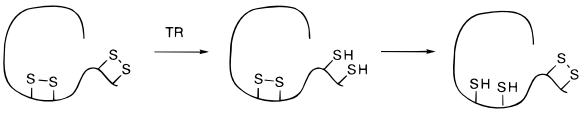

(1)

These cysteines can then in turn shuttle the reducing equivalents into the active site during another round of dithiol interchange. Alternatively, low-molecular mass thiols such as dithiothreitol (DTT) can bypass cysteines 754 and 759 and directly reduce the disulfide between Cys225 and Cys462.

Several different strategies for inactivation of RNRs have been reported, including the use of substrate analogues as mechanism-based inhibitors (*16*−*21*). Over the past 15 years, RDPR inactivation by many 2′-substituted nucleotide analogues has been studied in detail, and a paradigm has been developed for their mechanism of inhibition (*16*, *22*). In general, inactivation occurs by partitioning between reduction of the essential $Y^{\bullet}$ on the R2 subunit and alkylation of critical residues of the R1 subunit. Studies by Reichard and Fontecave and their co-workers with *E. coli* have shown that loss of the $Y^{\bullet}$ can be reversed by the action of a flavodoxin reductase and an unknown factor in the presence of O_2 (*23*, *24*). Thus, although at present it is unclear whether such a pathway exists in mammalian cells, it appears that therapeutic inhibitors of RNR that target both subunits may be clinically most effective. With most 2′-substituted nucleotide analogues studied to date, R1 inactivation can be prevented by the addition of low-molecular mass nucleophiles such as DTT. Presented here are studies on the mechanism of inactivation of RDPR from *E. coli* by **1** that demonstrate that 1 equiv of this compound inhibits R1 in the presence of DTT, whereas R2 is inactivated in the absence of DTT. Furthermore, these studies show that under certain conditions a new stable radical is formed.

MATERIALS AND METHODS

Materials. R1 (ϵ_{280nm} = 189 000 M^{-1} cm^{-1}), with a specific activity (SA) of 1500∼1700 nmol min^{-1} mg^{-1}, and R2 (ϵ_{280nm} = 130 500 M^{-1} cm^{-1}) with a SA of 7700∼8000 nmol min^{-1} mg^{-1} (*25*), prereduced R1 and oxidized R1 (*26*), and the R1 mutant C754S/C759S isolated from an *E. coli* K38 overproducing strain (*13*) were all prepared as previously described. *E. coli* TR was isolated from SK3981 (*27*)-with a SA of 36 units mg^{-1}, and TRR was isolated from K91/pMR14 (*28*) with a SA of 1000 units mg^{-1}. Calf intestine alkaline phosphatase was purchased from Boehringer Mannheim. Adenosine 5′-triphosphate (ATP) and reduced β-nicotinamide adenine dinucleotide phosphate (β-NADPH) were obtained from Sigma. DTT was purchased from Mallinckrodt. [U-^{14}C]CDP was purchased from New England Nuclear (SA of 532 mCi $mmol^{-1}$). The Hepes assay buffer contained 50 mM Hepes, 15 mM $MgSO_4$, and 1 mM EDTA (pH 7.6) unless indicated otherwise.

Methods. UV−vis spectroscopy was carried out using an HP8452A diode array spectrophotometer. Electron spin resonance (EPR) spectra at 9 GHz were acquired on a Bruker ESP-300 spectrometer at 100 K. Spin quantitation was achieved with a 1.0 mM $CuSO_4$, 2 M $NaClO_4$, 0.01 M HCl, and 20% (v/v) glycerol standard (g = 2.18) (*29*). Fluoride analyses were determined using an Orion 96−09 fluoride combination electrode using methods previously described (*30*). Liquid scintillation counting was performed on a Packard 1500 analyzer with Scint-A XF (Packard) scintillation fluid. HPLC for product analysis was performed on a Beckman System 110B with an Alltech Econosil C18 column (4 mm × 25 cm, 10 μm).

Time-Dependent Loss of $Y^{\bullet}$ and R1 Activity. The inactivation reaction was carried out in a cuvette at 25 °C containing 15 μM R1, 15 μM R2, 1.6 mM ATP, and 75 μM **1** in Hepes assay buffer. Reaction mixtures in the presence of external reductants contained 10 mM DTT, or 10 μM TR, 0.5 μM

TRR, and 1 mM NADPH. Time-dependent loss of the Y• was monitored by the change in A_{412nm} using the previously reported drop-line correction at 412 nm [$A_{412} - (2A_{406} + 3A_{416})/5$], with an ϵ of 1920 M^{-1} cm^{-1} (*31*). Simultaneously, inactivation of R1 was monitored by removing 5 μL aliquots at various time points which were diluted with 20 μL of Hepes buffer, and 5 μL of this solution was added to 95 μL of an assay solution containing 75 μM R2 (a 6-fold molar excess of R2 over R1), 1.0 mM [U-^{14}C]CDP (SA of 1.1 × 10^6 cpm/μmol), 1.6 mM ATP, 1.0 mM NADPH, 10 μM TR, 0.5 μM TRR, and Hepes assay buffer. The reactions were quenched after 5 min by immersion in a boiling water bath. The reaction mixture was made 0.16 M in Tris·HCl (pH 8.0), treated with 5 units of *E. coli* alkaline phosphatase, and incubated at 37 °C for 1.5 h. Carrier deoxycytidine (dC, 80 nmol) was added, and the dC was quantitated by the method of Steeper and Steuart (*32*).

Identification of Products Accompanying Inactivation of RDPR. RDPR (15 μM) was incubated, typically for 30 min at 25 °C, with **1** under the conditions described above in a final volume of 1.8 mL. The low-molecular mass components were separated from the proteins with Centricon-30 instruments, and the protein solution was washed once with 1 mL of 50 mM Hepes assay buffer (pH 7.6). The combined filtrates were lyophilized, and the residue was dissolved in 1 mL of water. The fluoride content was determined as previously described (*30*).

After analysis for fluoride, 250 μL of 0.5 M Tris buffer (pH 8.4) and 5 units of calf intestine alkaline phosphatase were added to the mixture and the mixture was incubated for 2 h at 37 °C. The mixture was then passed through a 0.5 × 10 cm Dowex anion exchange column in the tetraborate form (*32*). The column was eluted with 10 mL of water, the resulting solution lyophilized, and the residue redissolved in 500 μL of water. The sample was then chromatographed on an Econosil C-18 Alltech RP column at a flow rate of 1.0 mL min^{-1} using isocratic elution with 5 mM potassium phosphate buffer (pH 6.8) for 10 min, followed by a linear gradient to 30% methanol/70% phosphate buffer over the course of 30 min. Retention times were as follows: cytosine, 5 min; and gemcitabine, 25 min. Cytosine was identified and quantitated by its characteristic shift in λ_{max} from 267 nm (ϵ = 6600 M^{-1} cm^{-1}) to 276 nm (ϵ = 9100 M^{-1} cm^{-1}) when the pH was changed from 6.8 to 1.6, respectively.

Time-Dependent Release of Fluoride. The release of fluoride during the inactivation of RDPR by **1** was monitored using a fluoride electrode inserted into the reaction vessel. The sample contained, in a final volume of 1 mL, 25 μM prereduced R1, 25 μM R2, 1.6 mM ATP, and 50 mM Hepes assay buffer (pH 7.6). TR, TRR, and NADPH were omitted from the assay since they were found to interfere with the electrode readings (data not shown). An aliquot of a stock NaF solution was then added to the solution to give a final concentration of 75 μM. This provided a constant initial electrode reading and ensured that the fluoride concentrations measured were within the linear portion of a standard curve generated under identical conditions. In a control experiment, it was verified that this addition of fluoride did not affect the enzyme activity or its inactivation by **1**. The reaction was initiated by addition of **1** to a final concentration of 150 μM (6 equiv). The time-dependent change in electrode potential was recorded, and the fluoride content was determined from a calibration curve as previously described (*30*). The time dependence of the reduction of Y• was examined in a parallel experiment under identical conditions by monitoring its A_{410nm} (*31*). At t = 180 s, an aliquot was withdrawn from the second sample, transferred to an EPR tube, and frozen in liquid N_2. This sample was analyzed by EPR spectroscopy as described below.

Two control experiments were carried out. First, it was verified that the release of fluoride was enzyme-dependent by performing the reaction with R2 that had been inactivated by reduction of Y• with 15 mM hydroxyurea for 20 min. Second, the dead time of the electrode response was determined under the conditions of the assay described above. Aliquots of NaF stock solution were added to a solution of the same composition as described above, and the electrode reading was followed as a function of time. The response could be fitted to a first-order process with a rate constant of 0.09 ± 0.02 s^{-1}.

*9 GHz EPR Studies on the Interaction of **1** with RDPR.* A spectrum of the Y• was recorded before addition of the inhibitor as described in the legend of Figure 5. This sample contained, in a final volume of 250 μL, 75 μM prereduced R1, 75 μM R2, 1.6 mM ATP, and 50 mM Hepes assay buffer (pH 7.6). The reaction was initiated by addition of **1** to a final concentration of 300 μM. Reactions carried out in the presence of external reducing equivalents contained 10 mM DTT as a reductant, or 4.5 μM TR, 0.2 μM TRR, and 0.5 mM NADPH. The reaction mixtures were incubated aerobically at 25 °C for various amounts of time, transferred to an EPR tube, and frozen in liquid nitrogen. To obtain spectra of new paramagnetic intermediates, the signal of Y• was subtracted from the experimentally acquired spectra as described previously (*33*). For the experiments performed in ^2H_2O, RDPR was passsed through a 1.5 × 25 cm G-25 Sephadex column equilibrated and eluted with Hepes assay buffer in ^2H_2O (pD 7.6).

The power dependence of the signal amplitude of the new radical was obtained from spectra recorded at various microwave powers and subsequent subtraction of the signal of Y• recorded under the same experimental conditions. The data so obtained were fitted to eq 2 (*34*, *35*)

$$\log(A/\sqrt{P}) = \log K - 0.5b \log[1 + (P/P_{1/2})] \quad (2)$$

in which I is the integrated intensity of the first-derivative (modulation detected) EPR spectrum, P is the parametrically varied microwave power, K is a sample and instrument-dependent parameter, b gauges the type of spectral broadening (homogeneous vs inhomogeneous) (*36*, *37*), and $P_{1/2}$ is the microwave power at half-saturation of the EPR signal.

Preparation of [U-^{2}H]R1. Uniformly deuterium-labeled R1 was obtained from *E. coli* strain BL21 DE3 carrying the plasmid pMJ1 (*13*) that was grown in Davis minimal media in D_2O with deuterated succinic acid as the sole carbon source. The bacteria were adapted to growth in D_2O by incubation of five successive generations in 25, 50, 75, 90, and 100% D_2O-containing Davis medium, respectively. Overexpression of R1 was obtained by induction of a 1 L culture that had reached an optical density (OD) of 1 at 37 °C with 1 mM IPTG. The cells were harvested after an additional 10 h. R1 was prepared as described previously,

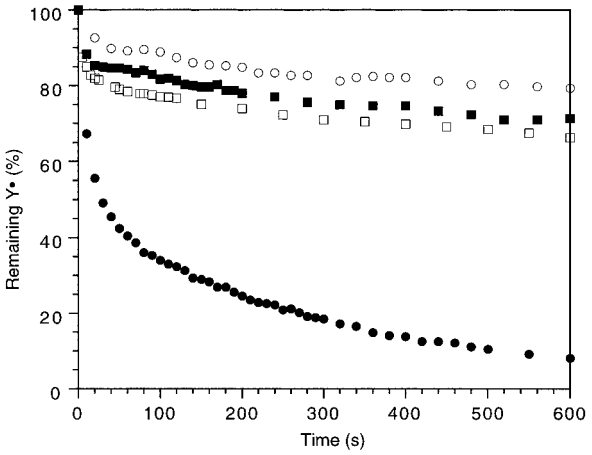

FIGURE 1: Time-dependent reduction of the Y• on R2 during the reaction of RDPR with **1**. Conditions were as follows: [prereduced R1] and [R2] = 15 μM, [**1**] = 75 μM, [ATP] = 1.6 mM, and with (○) 75 μM TR, 0.8 μM TRR, and 0.5 mM NADPH, (■) 10 mM DTT, or (□) 3 μM TR, 0.5 μM TRR, and 0.5 mM NADPH, or (●) without any external reductants.

providing 4 mg of protein (SA of 800 nmol min^{-1} mg^{-1}). To confirm the incorporation of deuterium into R1, the protein was incubated with R2, N_3UDP, and ATP as described previously (*38*), the reaction mixture was frozen after 5 min, and an EPR spectrum was recorded. The spectrum clearly showed the absence of a proton hyperfine interaction that was present in a control with protonated R1, and which has been previously shown to be derived from a β-proton on a cysteine residue of R1 (*38*).

RESULTS

The Mode of Inactivation Is Reductant-Dependent. As discussed above, RDPR inactivation generally involves reduction of the essential Y•, alkylation of R1, or both. To investigate the mode of inactivation by **1**, the characteristic absorbance of the Y• at 410 nm was monitored during the reaction of RDPR with 5 equiv of the inhibitor. In the presence of TR, TRR, and NADPH, loss of about 10% of the Y• signal was observed in the first 30 s of the reaction (Figure 1), followed by a much slower phase ultimately leading to ~25% reduction of Y• after 15 min. Nucleotide reduction activity was completely abolished at this time point (data not shown). The extent of Y• reduction was not dependent on the RDPR:TR ratio as both excess and substoichiometric quantities of TR gave similar results (Figure 1). However, when either TR, TRR, or NADPH was omitted from the inactivation reaction, complete loss of Y• was observed (data not shown). Complete destruction of the radical was also observed when prereduced RDPR was incubated with 5 equiv of **1** in the absence of any reducing equivalents (Figure 1). In contrast, partial loss of Y• was observed in the presence of 10 mM DTT, conditions under which RDPR is completely inactivated as demonstrated in previous studies (*9*). Thus, these results suggest that, in the absence of reducing equivalents, RDPR inactivation is at least partly due to reduction of Y•, while in the presence of reductants, enzyme inhibition must occur predominantly by a different mechanism.

As mentioned above, certain mechanism-based inhibitors achieve their inhibitory action of RDPR by covalent alkylation of critical residues of the R1 subunit. Previous studies with 2′-deoxy-2′-halonucleotides have provided evidence that release of halide and nucleic base produces an electrophilic furanone derivative **2** that is responsible for this covalent labeling and that trapping of this intermediate by a nucleophilic group on R1 produces a chromophore around 320−330 nm (*39*). Inactivation of R1 by this pathway can be prevented by addition of thiols such as ethanethiol or DTT which trap the furanone, **2**.

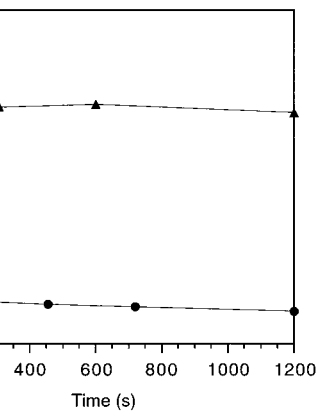

FIGURE 2: Time-dependent inactivation of R1 by **1**. Conditions were as follows: [prereduced R1] and [R2] = 15 μM, [**1**] = 75 μM, [ATP] = 1.6 mM, and (▲) no external reductants or (●) in the presence of 15 μM TR, 0.5 μM TRR, and 1.0 mM NADPH.

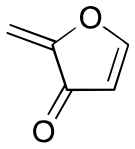

2

To investigate whether R1 is inactivated by **1**, aliquots of the inactivation mixtures were removed and diluted into an assay solution containing a 6-fold molar excess of R2. As shown in Figure 2, fast and complete inactivation of the R1 subunit was observed in the presence of TR/TRR/NADPH, i.e., under conditions where Y• on R2 is only partially affected (Figure 1). When prereduced RDPR was reacted with **1** in the absence of external reductants, a fast loss of 50% of the R1 activity was observed, followed by a recovery to about 70% of the original activity. Analysis of RDPR after removal of the low-molecular mass reactants by gel filtration chromatography revealed the absence of any chromophore associated with the protein. Furthermore, addition of DTT did not prevent R1 inactivation. Thus, it appears that **1** inactivates R1 by a different mechanism than all previously studied 2′-substituted nucleotide analogues except 2′-fluoromethylene 2′-deoxycytidine 5′-diphosphate (FMCDP). In this case, we have recently shown that R1 is stoichiometrically and covalently modified both in the presence and in the absence of DTT (*22*). We are presently synthesizing [^{3}H]-**1** to address the question of whether a covalent adduct to R1 is formed which does not produce an associated chromophore.

*Reaction of **1** with C754S/C759S-R1*. The results described above show that the characteristics of RDPR inactivation change dramatically depending on the presence or absence of reductants. Cysteines 754 and 759 on R1 have

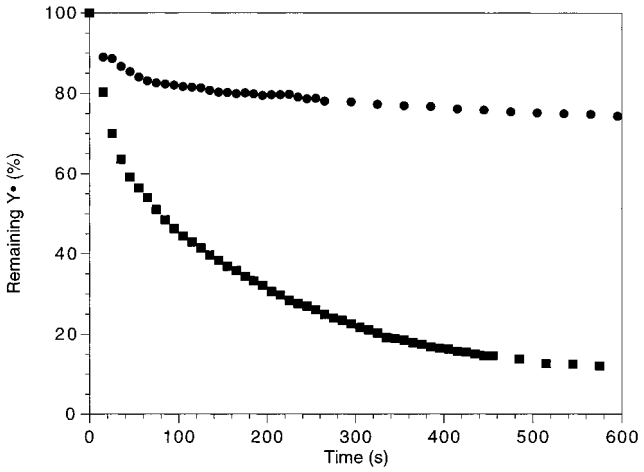

FIGURE 3: Time-dependent reduction of the Y• on R2 during the incubation of C754S/C759S-R1, R2, and **1**. Conditions were as follows: [prereduced C754S/C759S-R1] and [R2] = 15 μM, [**1**] = 75 μM, [ATP] = 1.6 mM, and (■) 15 μM TR, 0.5 μM TRR, and 0.5 mM NADPH, or (●) 10 mM DTT.

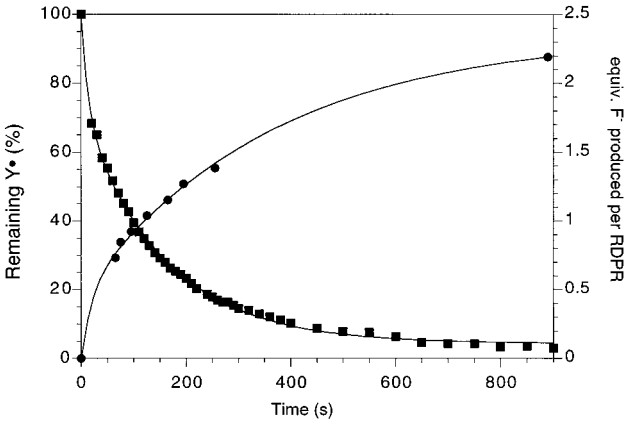

FIGURE 4: Time dependence of fluoride release (●) and loss of the Y• absorbance at 410 nm (■) during the inactivation of RDPR with **1**. Linear regression fits of the data to double-exponential equations are indicated by the solid lines through the data points.

been proposed to function as key components of a relay system that shuttles reducing equivalents from TR into the active site (*12*, *13*). Site-directed mutagenesis studies have shown that mutation of these residues to serines produces a protein that lacks the ability to catalyze multiple turnovers, supporting this hypothesis. Small thiol reductants such as DTT, however, can support multiple turnovers of this mutant protein, suggesting that these reductants are able to bypass the block in the relay system imposed by mutation of C754 and C759. Thus, to investigate whether the reversal of the target of inactivation by TR/TRR/NADPH or DTT involves the delivery of reducing equivalents into the active site, the double mutant C754S/C759S-R1 was incubated with **1**. As shown in Figure 3, both in the absence of external reducing equivalents (data not shown) and in the presence of TR/TRR/NADPH, complete loss of the Y• was observed. When DTT was present in the reaction mixture, however, the time dependence of the Y• reduction was very similar to that observed with wt-R1.

Identification of Products Accompanying RDPR Inactivation. Previous studies with 2′-deoxy-2′-halonucleotides have demonstrated that inactivation of RDPR is accompanied by nucleic acid base and halide release into solution (*14*, *16*). To characterize the products formed with **1**, the protein was separated from low-molecular mass compounds by means of centrifugation through a membrane with a 30 kDa cutoff. The resulting filtrates were analyzed for fluoride ion and cytosine content and compared to control samples in which R2 had been replaced with met-R2 (R2 in which Y• has been reduced with hydroxyurea). The results indicate that 2 equiv of fluoride and 1 equiv of cytosine were produced per RDPR inactivated irrespective of the presence or absence of external reducing agents. Quantitation of recovered inhibitor revealed that one molecule of **1** is consumed during the inactivation. Thus, cytosine and both fluorides are released from the sugar moiety of **1**. The fate of the ribose itself is at present unknown.

To examine the time scale on which the two fluorides are released with respect to inactivation, the fluoride concentration in the inactivation mixture was monitored using a fluoride electrode during incubation of RDPR with 6 equiv of **1**. As shown in Figure 4, the reaction produced 2 equiv of fluoride per equivalent of Y• reduced as determined by monitoring an absorbance change at 410 nm (*31*). A control experiment in which R2 was inactivated by reduction of Y• (met-R2) indicated that this fluoride release is enzyme-dependent (data not shown). The data for the time-dependent increase in fluoride concentration were fit to a double-exponential equation using nonlinear regression analysis, providing apparent first-order rate constants of $(5.0 \pm 4.8) \times 10^{-2}$ and $(0.30 \pm 0.25) \times 10^{-2}$ s^{-1}. In a control experiment, it was established that the response time of the electrode was about 2 times faster than the observed rate of fluoride release. Therefore, the data reported here represent a lower limit for the rate of fluoride production.

Finally, the rate of fluoride release has been compared with the rate of reduction of the Y• under identical conditions (Figure 4). The rate of loss of Y• can be fit to a double-exponential equation with rate constants of $(7.5 \pm 0.9) \times 10^{-2}$ and $(0.64 \pm 0.17) \times 10^{-2}$ s^{-1}. These results thus indicate that reduction of Y• occurs at approximately the same rate as the release of fluoride, and thus could be a prerequisite for this process.

*EPR Studies on the Interaction of **1** with RDPR.* Studies on the interaction of 2′-azido-2′-deoxyuridine 5′-diphosphate (N_3UDP) and FMCDP with RDPR have shown that rapid loss of Y• is accompanied by the generation of new, inhibitor-derived radicals (*18*, *22*, *40*). In the former case, this radical is nitrogen-based and covalently attached to a cysteine of R1 (*38*), and in the latter case, the radical is carbon-based and located on the nucleotide (*22*, *33*). Therefore, the observation of rapid loss of Y• in the absence of reducing equivalents (Figure 1) prompted us to investigate whether a new protein or nucleotide-based radical could be detected by EPR spectroscopy. A sample of RDPR (75 μM) was incubated with 4 equiv of **1** for 30 s and rapidly frozen at 77 K, and the EPR spectrum was recorded. As shown in Figure 5A, a new signal is observed which is different from that of Y• of R2 (Figure 5B). A closer examination of the spectrum in Figure 5A suggests that it is composed of two species, one being residual Y•. To obtain a spectrum of the new radical species, increasing amounts of the Y• signal were subtracted from the spectrum in Figure 5B, ultimately giving rise to the signal shown in Figure 5C.

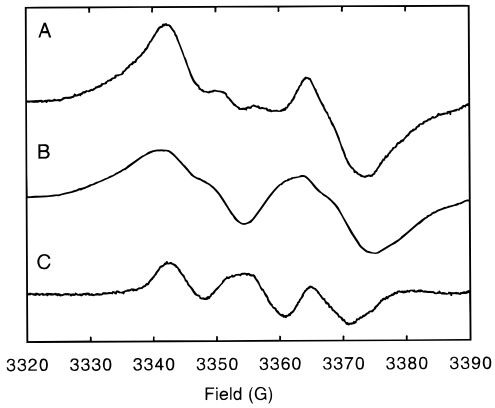

FIGURE 5: (A) 9.42 GHz EPR spectrum of a sample containing RDPR (75 μM), **1** (300 μM), and ATP (1.6 mM) frozen 30 s after addition of the inhibitor, (B) the EPR spectrum of $Y_{122}^{\bullet}$, and (C) the spectrum of the new radical intermediate at $t = 30$ s after subtraction of the contribution of the $Y_{122}^{\bullet}$ signal. Instrument settings for all spectra were as follows: power, 10 μW; modulation amplitude, 0.39 mT; time constant, 0.126 s; and temperature, 101 K.

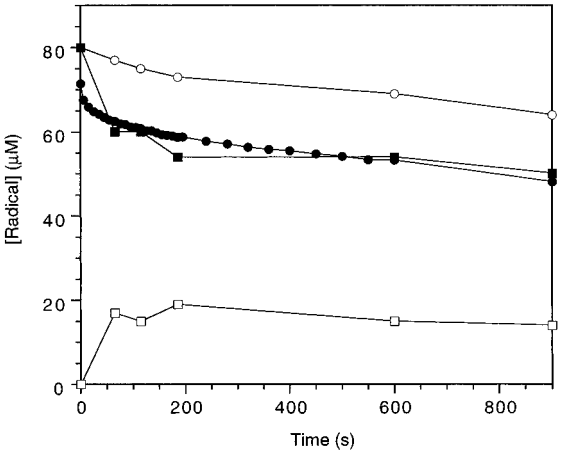

FIGURE 6: Time-dependent reduction of $Y^{\bullet}$ during the inactivation of RDPR by **1** monitored by (●) absorbance at 410 nm or (■) double integration of its EPR signal calibrated with a $CuSO_4$ standard of known concentration and (□) concentration of the new radical formed quantitated by EPR spectroscopy. (○) Total concentration of paramagnetic species present in the reaction mixture during the inactivation process.

Quantitation of the EPR signals shows that the amount of $Y^{\bullet}$ present at the 30 s time point is 60 ± 2 μM compared to 90 μM at $t = 0$ (1.2 $Y^{\bullet}$/RDPR) and that the new signal is present at 20 ± 2 μM.[2] Thus, the amount of new radical generated corresponds to about 65% of the amount of $Y^{\bullet}$ that is reduced. To further explore the time dependence of loss of $Y^{\bullet}$ and new radical formed, the $Y^{\bullet}$ content during the reaction was monitored by both UV−vis and EPR spectroscopy and compared with the amount of new radical formed. As is evident from the data in Figure 6, the new paramagnetic species is unusually stable for a period of more than 15 min. Furthermore, the amount of radical formed does not change appreciably after an initial fast generation. In fact, the amount of radical observed has been between 15 and 25% of the total enzyme under all experimental conditions investigated. The loss of $Y^{\bullet}$ at the concentrations used for these EPR studies is much slower in comparison with the inactivation studies described above (Figure 1). The R1 activity on the other hand was completely lost after 7 min under these conditions (data not shown). Thus, similar to the effect of reductants, relatively high protein concentrations induce a change in the partitioning between R1 and R2 inactivation.

To further probe the characteristics of the new signal, the microwave power dependence of its amplitude was investigated by subtraction of the $Y_{122}^{\bullet}$ signal from spectra obtained at various powers. These data provided a value of 1.0 ± 0.5 mW for $P_{1/2}$, the power at half-saturation (see Materials and Methods).[3] This value is about 1.5 orders of magnitude lower than that of the $Y^{\bullet}$ in R2 ($P_{1/2} = 47 \pm 12$ mW) (*33*). The electron spin relaxation rate of the latter is considerably enhanced compared to that of the free $Y^{\bullet}$ generated by irradiation of a frozen solution ($P_{1/2} = 0.64 \pm 0.19$ mW, $b = 1.48 \pm 0.17$) (*41*), due to its proximity to the diferric cluster. Overall, the saturation behavior of the new radical suggests therefore that it is organic in nature and removed from the cluster.

To confirm the results of the saturation studies, and to further confine the possible origin of the EPR signal, **1** was reacted with uniformly deuterated R1. This experiment resulted in the production of EPR signals identical to that shown in Figure 5, indicating that the observed hyperfine structure is not derived from nonexchangeable protons on R1 (data not shown). In addition, reactions performed in D_2O did not perturb the signal, ruling out the involvement of solvent exchangeable protons (data not shown).

*EPR Studies on the Reaction of **1** with RDPR Containing Oxidized R1 or C754S/C759S-R1.* As shown in Figure 3, the reaction of **1** with C754S/C759S-R1 leads to rapid loss of $Y^{\bullet}$. EPR analysis of this reaction showed a new radical species identical to that produced with wild-type R1 (data not shown). Once again, the radical was produced in about 20−25% of the total enzyme concentration. Thus, cysteines 754 and 759 are not involved in generation of this radical. Interestingly, this mutant R1 did not show the decrease in the rate of $Y^{\bullet}$ loss at higher protein concentrations that was observed with wild-type R1.

To investigate the requirement of Cys225 and Cys462 in the active site of R1 for the formation of the radical species, **1** was incubated with R1 in which these cysteines had been oxidized to the disulfide. Rapid and complete loss of the $Y^{\bullet}$ was observed to be concomitant with the production of an EPR signal identical to that observed with prereduced R1 (data not shown). Therefore, having these thiols in their reduced state is not required for the formation of this paramagnetic species.

DISCUSSION

Mode of Inactivation. The characteristics of the inactivation of RDPR from *E. coli* by the clinically important nucleotide analogue **1** are presented in eq 3.

[2] The errors reflect differences in the subtractions. While the experiments were carried out multiple times, they were not carried out under identical conditions, and hence, quantitation of the EPR signal intensity error has not been included. In all cases, the new radical signal accounted for 65−70% of the $Y^{\bullet}$ signal lost.

[3] The relatively large error in the value for $P_{1/2}$ is most likely due to the low singal-to-noise ratios of the difference spectra obtained at both low and high microwave powers.

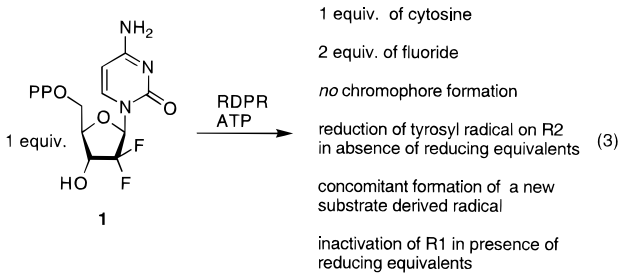

(3)

Quantitation of the products of the reaction indicate that 1 equiv of **1** is consumed per equivalent of RDPR inactivated and that cytosine and both fluorides are released into solution. The data shown in Figures 2 and 3 suggest that during this process **1** targets predominantly R1 in the presence of external reductants, while in the absence of reductants, its inhibitory action is predominantly due to reduction of Y• on R2. Reductant-dependent partitioning between two inactivation pathways has been observed previously with other 2′-substituted nucleotide mechanism-based inhibitors of RDPR (*20*). However, the results of those previous studies showed that the presence of low-molecular mass reductants (such as DTT) prevented R1 inactivation, while in the case of **1**, the presence of reductants (either thiols or TR/TRR/NADPH) is required for R1 inhibition. In addition, the formation of a chromophore, characteristic of other 2′-substituted nucleotide inhibitors, is not observed in the case of **1**. Thus, R1 inactivation by **1** is probably not due to a furanone-type reactive intermediate generated in solution. The chemistry of chromophore formation during inactivation of both class I and II RNRs by 2′-substituted 2′-deoxynucleotides is thought to arise by alkylation of the C-terminal cysteines, C754 or C759 in *E. coli*, by **2** generated in solution, which then reacts with a conserved lysine, K760, at the C terminus of R1. In contrast, it could be in the case of **1** that the chemistry occurs within the active site cavity. As no lysine is within the vicinity of the active site on the basis of the structure of R1 (*15*), alkylation could occur without chromophore formation.

An excess of DTT or a substoichiometric amount of the enzymatic reduction system of TR/TRR/NADPH prevents Y• loss, but when TRR or NADPH is omitted, complete reduction of Y• is observed. These results suggest that these reagents may induce this change by performing a reductive step during the inactivation. Three additional observations are consistent with such a scenario. First, complete loss of the Y• is observed in the reaction of **1** with RDPR containing the mutant C754S/C759S-R1 in the presence of TR/TRR/NADPH. This mutant is unable to receive reducing equivalents from TR and thus cannot reduce any disulfide formed between Cys225 and -462 in the active site of R1. Second, incubation of C754S/C759S-R1, R2, and **1** in the presence of DTT did not lead to complete loss of Y•, but rather showed a behavior similar to that of wild-type RDPR. Since previous studies have shown that DTT can directly reduce the disulfide formed in the active site between Cys225 and -462 in this mutant, these results are consistent with but do not prove that delivery of reducing equivalents to the active site alters the target of inactivation by **1** from R2 to R1. Finally, one additional observation supports this hypothesis. The rate of Y• loss in the absence of reducing equivalents is slowed at higher protein concentrations (Figure 6), a behavior not observed for the mutant C754S/C759S-R1. In previous studies, Mao et al. (*13*) suggested not only that Cys754 and Cys759 may serve as an intramolecular shuttle but also that under certain conditions these cysteines may act as an intermolecular reducing agent. They can function in a fashion similar to that of the redox active cysteines of thioredoxin, albeit at a slower rate. This postulate would explain why wild-type RDPR at high protein concentrations behaves more as if TR/TRR/NADPH were present, while C754S/C759S-R1 does not display this behavior. At present, it is clear that the mechanism(s) of inactivation of RDPR by **1** is efficient, but chemically complex. Further experiments, as described above, are required to propose a reasonable hypothesis for this process(es).

What Is the Structure of the New Radical? The EPR studies presented here demonstrate the formation of an unusually stable radical species whose formation is only observed in the absence of reducing equivalents. This radical is formed in the initial fast phase of inactivation of R2 but never exceeds 25% of the total enzyme concentration. Thus, this radical species accounts for only a minor part of the R2 inactivation process.

The power saturation studies suggest that the radical is distant to the diferric center and is organic in nature. Docking experiments of the crystal structures of the R1 and R2 subunits of RDPR have suggested that the active site on R1 is ∼35 Å from the diferric cluster−Y• cofactor located on R2 (*15*). Thus, a substrate-derived radical in the active site of R1 is a possible candidate for the observed paramagnetic species. The overall appearance of the signal is that of a triplet pattern with unequal intensities. Recall that the signal is obtained by subtraction of the signal of the Y• acquired under the same conditions. Such a signal could be produced by hyperfine interaction of the unpaired electron with two nuclei with $I = {}^1/_2$, such as protons or fluorides, or to one $I = 1$ nucleus such as ^{14}N. The magnitude of the observed hyperfine interaction **(**∼1.2 to 1.3 mT**)**, however, is inconsistent with a fluorine located α or β to the radical site which produce hyperfine interactions of >3.0 mT (*42*). Although at present we cannot rule out ^{14}N, the asymmetry of the signal appears to support that it is the result of two overlapping doublet signals. Thus, it seems most likely that two protons give rise to the observed hyperfine pattern. Studies with [U-^{2}H]R1 and in ^2H_2O rule out the possibility that these hyperfine interactions are derived from protons on R1 or from solvent. Synthesis of 1′-^{2}H- and 5′-^{2}H-labeled **1** is currently underway to investigate the structure of the radical intermediate (*43*).[4]

Summary. Gemcitabine 5′-diphosphate is the most potent mechanism-based inhibitor of RDPR studied to date. The mechanism responsible for inactivation partitions between loss of R1 and R2 depending on the presence or absence of reductant, respectively. Inside the cell, it is likely that reductant is in fact accessible; hence, R1 inactivation is the most reasonable target and is proposed to contribute to the drug's cytotoxicity. R1 as a target is appealing, given the lability of the diferric−Y• cofactor in eukaryotic systems and

[4] While this work was being reviewed, a paper appeared that describes two new radical species observed when a mutant of R1, E441Q, interacts with CDP, the normal substrate. The signal of the "stable" radical appears to be similar to that described here.

its ease of regeneration (*44*). Stoichiometric inactivation of R1 (probably by covalent modification) is distinct from the majority of those of the other 2′-substituted 2′-deoxynucleotides, suggesting that the reactive species is generated within the R1 active site and never leaves this site even though reductant is required. In vitro, when reductant is absent, the loss of the Y• is responsible for inactivation. Approximately 15−25% of the time, this pathway generates a nucleotide-based radical. From available evidence thus far, the structure of this radical is unusual given our understanding of reductase chemistry. Its characterization will give us, once again, new insight into the unique chemistry of this radical enzyme with suicidal tendencies.

REFERENCES

1. Abratt, R. P. (1995) *Anti-Cancer Drugs 6*, 63−64.
2. Hertel, L. W., Kroin, J. S., Grossman, C. S., Grindey, G. B., Dorr, A. F., Storniolo, A. M. V., Plunkett, W., Gandhi, V., and Huang, P. (1996) *ACS Symp. Ser. 639*, 265−278.
3. Gandhi, V., and Plunkett, W. (1989) *Proc. Am. Assoc. Cancer Res. 30*, 589.
4. Shewach, D. S., Reynolds, K. K., and Hertel, L. (1992) *Mol. Pharmacol. 42*, 518−524.
5. Plunkett, W., Huang, P., Xu, Y.-Z., Heinemann, V., Grunewald, R., and Gandhi, V. (1995) *Semin. Oncol. 22*, 3−10.
6. Heinemann, V., Xu, Y.-Z., Chubb, S., Sen, A., Hertel, L., Grindey, G. B., and Plunkett, W. (1989) *Proc. Am. Assoc. Cancer Res. 30*, 554.
7. Heinemann, V., Xu, Y.-Z., Chubb, S., Sen, A., Hertel, L. W., Grindey, G. B., and Plunkett, W. (1990) *Mol. Pharmacol. 38*, 567−572.
8. Huang, P., Chubb, S., Hertel, L. W., Grindey, G. B., and Plunkett, W. (1991) *Cancer Res. 51*, 6110−6117.
9. Baker, C. H., Banzon, J., Bollinger, J. M., Jr., Stubbe, J., Samano, V., Robins, M. J., Lippert, B., Jarvi, E., and Resvick, R. (1991) *J. Med. Chem. 34*, 1879−1884.
10. Thelander, L. (1974) *J. Biol. Chem. 249*, 4858−4862.
11. Lin, A. I., Ashley, G. W., and Stubbe, J. (1987) *Biochemistry 26*, 6905−6909.
12. Åberg, A., Hahne, S., Karlsson, M., Larrson, Å., Ormö, M., Åhgren, A., and Sjöberg, B. M. (1989) *J. Biol. Chem. 264*, 2249−2252.
13. Mao, S. S., Holler, T. P., Yu, G. X., Bollinger, J. M., Booker, S., Johnston, M. I., and Stubbe, J. (1992) *Biochemistry 31*, 9733−9743.
14. Stubbe, J. (1990) *J. Biol. Chem. 265*, 5329−5332.
15. Uhlin, U., and Eklund, H. (1994) *Nature 370*, 533−539.
16. Stubbe, J., and van der Donk, W. A. (1995) *Chem. Biol. 2*, 793−801.
17. Thelander, L., Larsson, B., Hobbs, J., and Eckstein, F. (1976) *J. Biol. Chem. 251*, 1398−1405.
18. Sjöberg, B.-M., Gräslund, A., and Eckstein, F. (1983) *J. Biol. Chem. 258*, 8060−8067.
19. Cory, J. G., and Cory, A. H., Eds. (1989) *Inhibitors of Ribonucleotide Diphosphate Reductase Activity*, Pergamon Press, New York.
20. Stubbe, J. (1990) *Adv. Enzymol. Relat. Areas Mol. Biol. 63*, 349−417.
21. Robins, M. J., Samano, M. C., and Samano, V. (1995) *Nucleosides Nucleotides 14*, 485−493.
22. van der Donk, W. A., Yu, G., Silva, D. J., Stubbe, J., McCarthy, J. R., Jarvi, E. T., Matthews, D. P., Resvick, R. J., and Wagner, E. (1996) *Biochemistry 35*, 8381−8391.
23. Fontecave, M., Eliasson, R., and Reichard, P. (1987) *J. Biol. Chem. 262*, 12325−12331.
24. Fontecave, M., Nordlund, P., Eklund, H., and Reichard, P. (1992) *Adv. Enzymol. Relat. Areas Mol. Biol. 65*, 147−183.
25. Salowe, S. P., and Stubbe, J. (1986) *J. Bacteriol. 165*, 363−366.
26. Salowe, S. P., Bollinger, J. M., Jr., Ator, M., Stubbe, J., McCracken, J., Peisach, J., Samano, M. C., and Robins, M. J. (1993) *Biochemistry 32*, 12749−12760.
27. Lunn, C. A., Kathju, S., Wallace, B. J., Kushner, S., and Pigiet, V. (1984) *J. Biol. Chem. 259*, 10469−10474.
28. Russell, M., and Model, P. (1985) *J. Bacteriol. 163*, 238−242.
29. Malmström, B., Reinhammar, B., and Vänngård, T. (1970) *Biochim. Biophys. Acta 205*, 48.
30. Stubbe, J., and Kozarich, J. W. (1980) *J. Biol. Chem. 255*, 5511−5513.
31. Bollinger, J. M., Jr., Edmonson, D. E., Huynh, B. H., Filley, J., Norton, J. R., and Stubbe, J. (1991) *Science 253*, 292−298.
32. Steeper, J. R., and Steuart, C. D. (1970) *Anal. Biochem. 34*, 123−130.
33. Gerfen, G. J., van der Donk, W. A., Yu, G., Farrar, C., Griffin, R. G., Stubbe, J., McCarthy, J. R., Matthews, D. P., and Jarvi, E. T. (1998) *J. Am. Chem. Soc.* (in press).
34. Beinert, H. (1972) in *Biological Applications of Electron Spin Resonance* (Swartz, H. M., and Bolton, J. R., Eds.) Wiley-Interscience, New York.
35. Rupp, H., Rao, K. K., Hall, D. O., and Cammack, R. (1978) *Biochim. Biophys. Acta 537*, 255−269.
36. Portis, A. M. (1953) *Phys. Rev. 91*, 1071.
37. Castner, T. G., Jr. (1959) *Phys. Rev. 115*, 1506.
38. van der Donk, W. A., Stubbe, J., Gerfen, G. J., Bellew, B. F., and Griffin, R. G. (1995) *J. Am. Chem. Soc. 117*, 8908−8916.
39. Harris, G., Ator, M., and Stubbe, J. (1984) *Biochemistry 23*, 5214−5225.
40. Ator, M., Salowe, S. P., Stubbe, J., Emptage, M. H., and Robins, M. J. (1984) *J. Am. Chem. Soc. 106*, 1886−1887.
41. Chen-Barrett, Y., Harrison, P. M., Treffry, A., Quail, M. A., Arosio, P., Santambrogio, P., and Chasteen, N. D. (1995) *Biochemistry 34*, 7847−7853.
42. Iwasaki, M. (1971) in *Fluorine Chemistry Reviews* (Tarrant, P., Ed.) Marcel Dekker, New York.
43. Persson, A. L., Eriksson, M., Katterle, F., Potsch, S., Sahlin, M., and Sjoberg, B. M. (1997) *J. Biol. Chem. 272*, 31533−31541.
44. Nyholm, S., Mann, G. J., Johansson, A. G., Bergeron, R. J., Graeslund, A., and Thelander, L. (1993) *J. Biol. Chem. 268*, 26200−26205.

BI9729357